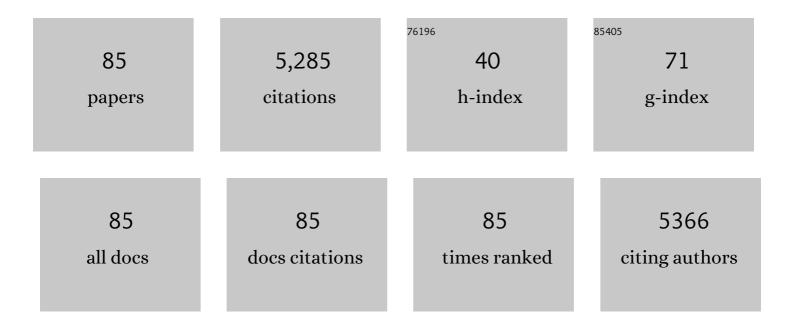
List of Publications by Year in descending order

Source: https://exaly.com/author-pdf/2711110/publications.pdf Version: 2024-02-01



SHIELL CHEN

#	Article	IF	CITATIONS
1	Study on the separation mechanisms of photogenerated electrons and holes for composite photocatalysts g-C3N4-WO3. Applied Catalysis B: Environmental, 2014, 150-151, 564-573.	10.8	572
2	Design of a direct Z-scheme photocatalyst: Preparation and characterization of Bi2O3/g-C3N4 with high visible light activity. Journal of Hazardous Materials, 2014, 280, 713-722.	6.5	344
3	Coupled systems for selective oxidation of aromatic alcohols to aldehydes and reduction of nitrobenzene into aniline using CdS/g-C3N4 photocatalyst under visible light irradiation. Applied Catalysis B: Environmental, 2014, 158-159, 382-390.	10.8	255
4	Transforming type-I to type-II heterostructure photocatalyst via energy band engineering: A case study of I-BiOCI/I-BiOBr. Applied Catalysis B: Environmental, 2017, 204, 505-514.	10.8	208
5	In situ preparation of novel p–n junction photocatalyst BiOI/(BiO)2CO3 with enhanced visible light photocatalytic activity. Journal of Hazardous Materials, 2012, 239-240, 316-324.	6.5	204
6	Selective oxidation of aromatic alcohols to aromatic aldehydes by BN/metal sulfide with enhanced photocatalytic activity. Applied Catalysis B: Environmental, 2016, 182, 356-368.	10.8	144
7	Ultra-low content of Pt modified CdS nanorods: one-pot synthesis and high photocatalytic activity for H ₂ production under visible light. Journal of Materials Chemistry A, 2015, 3, 23732-23742.	5.2	137
8	Photocatalytic reforming of glycerol for H ₂ evolution on Pt/TiO ₂ : fundamental understanding the effect of co-catalyst Pt and the Pt deposition route. Journal of Materials Chemistry A, 2015, 3, 2271-2282.	5.2	129
9	Efficient photocatalytic H2 evolution, CO2 reduction and N2 fixation coupled with organic synthesis by cocatalyst and vacancies engineering. Applied Catalysis B: Environmental, 2021, 285, 119789.	10.8	120
10	Preparation and characterization of direct Z-scheme photocatalyst Bi2O3/NaNbO3 and its reaction mechanism. Applied Surface Science, 2014, 292, 357-366.	3.1	119
11	One-step synthesis of 2D/2D-3D NiS/Zn3In2S6 hierarchical structure toward solar-to-chemical energy transformation of biomass-relevant alcohols. Applied Catalysis B: Environmental, 2020, 266, 118617.	10.8	115
12	One-pot hydrothermal synthesis of highly efficient SnOx/Zn2SnO4 composite photocatalyst for the degradation of methyl orange and gaseous benzene. Applied Catalysis B: Environmental, 2017, 200, 19-30.	10.8	112
13	Effective use of photogenerated electrons and holes in a system: Photocatalytic selective oxidation of aromatic alcohols to aldehydes and hydrogen production. Journal of Catalysis, 2018, 367, 159-170.	3.1	102
14	Efficient utilization of photogenerated electrons and holes for photocatalytic selective organic syntheses in one reaction system using a narrow band gap CdS photocatalyst. Green Chemistry, 2016, 18, 3628-3639.	4.6	101
15	Perspective on construction of heterojunction photocatalysts and the complete utilization of photogenerated charge carriers. Applied Surface Science, 2019, 476, 982-992.	3.1	101
16	Efficient utilization of photogenerated electrons and holes for photocatalytic redox reactions using visible light-driven Au/ZnIn2S4 hybrid. Journal of Hazardous Materials, 2019, 367, 277-285.	6.5	97
17	One-pot hydrothermal synthesis of BiPO4/BiVO4 with enhanced visible-light photocatalytic activities for methylene blue degradation. RSC Advances, 2014, 4, 10968.	1.7	94
18	In situ photodeposition of MoS _x on CdS nanorods as a highly efficient cocatalyst for photocatalytic hydrogen production. Journal of Materials Chemistry A, 2017, 5, 15287-15293.	5.2	93

#	Article	IF	CITATIONS
19	Simultaneous dehydrogenation and hydrogenolysis of aromatic alcohols in one reaction system via visible-light-driven heterogeneous photocatalysis. Journal of Catalysis, 2018, 357, 247-256.	3.1	91
20	Effect of different solvent on the photocatalytic activity of ZnIn2S4 for selective oxidation of aromatic alcohols to aromatic aldehydes under visible light irradiation. Applied Surface Science, 2016, 384, 161-174.	3.1	90
21	Synergistic effect of photocatalysis and thermocatalysis for selective oxidation of aromatic alcohols to aromatic aldehydes using Zn3In2S6@ZnO composite. Applied Catalysis B: Environmental, 2017, 218, 420-429.	10.8	90
22	Insight into the Transfer Mechanism of Photogenerated Carriers for WO ₃ /TiO ₂ Heterojunction Photocatalysts: Is It the Transfer of Band–Band or Z-Scheme? Why?. Journal of Physical Chemistry C, 2018, 122, 26326-26336.	1.5	88
23	Insight into the Transfer Mechanisms of Photogenerated Carriers for Heterojunction Photocatalysts with the Analogous Positions of Valence Band and Conduction Band: A Case Study of ZnO/TiO ₂ . Journal of Physical Chemistry C, 2018, 122, 15409-15420.	1.5	84
24	Rational synthesis of MnxCd1-xS for enhanced photocatalytic H2 evolution: Effects of S precursors and the feed ratio of Mn/Cd on its structure and performance. Journal of Colloid and Interface Science, 2019, 535, 469-480.	5.0	80
25	Chalcogenide photocatalysts for selective oxidation of aromatic alcohols to aldehydes using O2 and visible light: A case study of CdIn2S4, CdS and In2S3. Chemical Engineering Journal, 2018, 348, 966-977.	6.6	79
26	Photocatalytic degradation of benzene over different morphology BiPO4: Revealing the significant contribution of high–energy facets and oxygen vacancies. Applied Catalysis B: Environmental, 2019, 243, 780-789.	10.8	78
27	Trace Amount of SnO ₂ -Decorated ZnSn(OH) ₆ as Highly Efficient Photocatalyst for Decomposition of Gaseous Benzene: Synthesis, Photocatalytic Activity, and the Unrevealed Synergistic Effect between ZnSn(OH) ₆ and SnO ₂ . ACS Catalysis, 2016. 6. 957-968.	5.5	74
28	Solvothermal synthesis of CdIn2S4 photocatalyst for selective photosynthesis of organic aromatic compounds under visible light. Scientific Reports, 2017, 7, 27.	1.6	72
29	Controlled synthesis of Sn-based oxides via a hydrothermal method and their visible light photocatalytic performances. RSC Advances, 2017, 7, 27024-27032.	1.7	65
30	Self-Assembly of CdS/CdIn ₂ S ₄ Heterostructure with Enhanced Photocascade Synthesis of Schiff Base Compounds in an Aromatic Alcohols and Nitrobenzene System with Visible Light. ACS Applied Materials & Interfaces, 2019, 11, 46735-46745.	4.0	62
31	Constructing a system for effective utilization of photogenerated electrons and holes: Photocatalytic selective transformation of aromatic alcohols to aromatic aldehydes and hydrogen evolution over Zn3In2S6 photocatalysts. Applied Catalysis B: Environmental, 2019, 242, 302-311.	10.8	61
32	Noble metal-free 0D–1D NiS _x /CdS nanocomposites toward highly efficient photocatalytic contamination removal and hydrogen evolution under visible light. Dalton Transactions, 2018, 47, 12671-12683.	1.6	53
33	A new phosphidation route for the synthesis of NiP and their cocatalytic performances for photocatalytic hydrogen evolution over g-C3N4. Journal of Energy Chemistry, 2020, 48, 241-249.	7.1	51
34	Effect of Zn Vacancies in Zn ₃ In ₂ S ₆ Nanosheets on Boosting Photocatalytic N ₂ Fixation. ACS Applied Energy Materials, 2020, 3, 11275-11284.	2.5	49
35	Photocatalytic Performance of NiS/CdS Composite with Multistage Structure. ACS Applied Energy Materials, 2020, 3, 7736-7745.	2.5	48
36	Construction of novel S/CdS type II heterojunction for photocatalytic H 2 production under visible light: The intrinsic positive role of elementary α-S. Chemical Engineering Journal, 2017, 321, 484-494.	6.6	47

#	Article	IF	CITATIONS
37	Photocatalytic synthesis of Schiff base compounds in the coupled system of aromatic alcohols and nitrobenzene using CdXZn1â°'XS photocatalysts. Journal of Catalysis, 2018, 359, 151-160.	3.1	46
38	What Is the Transfer Mechanism of Photoexcited Charge Carriers for g-C ₃ N ₄ /TiO ₂ Heterojunction Photocatalysts? Verification of the Relative <i>p</i> – <i>n</i> Junction Theory. Journal of Physical Chemistry C, 2020, 124, 8561-8575.	1.5	46
39	Ultra-low content of Pt modified CdS nanorods: Preparation, characterization, and application for photocatalytic selective oxidation of aromatic alcohols and reduction of nitroarenes in one reaction system. Journal of Hazardous Materials, 2018, 360, 182-192.	6.5	45
40	Photocatalytic organic transformations: Simultaneous oxidation of aromatic alcohols and reduction of nitroarenes on CdLa2S4 in one reaction system. Applied Catalysis B: Environmental, 2018, 233, 1-10.	10.8	44
41	Novel S-scheme WO3/RP composite with outstanding overall water splitting activity for H2 and O2 evolution under visible light. Applied Surface Science, 2021, 558, 149882.	3.1	41
42	Investigation on the Mechanism and Inner Impetus of Photogenerated Charge Transfer in WO ₃ /ZnO Heterojunction Photocatalysts. Journal of Physical Chemistry C, 2020, 124, 27916-27929.	1.5	38
43	Construction of two-dimensionally relative p-n heterojunction for efficient photocatalytic redox reactions under visible light. Applied Surface Science, 2020, 505, 144638.	3.1	37
44	Efficient photocatalytic hydrogen production from formic acid on inexpensive and stable phosphide/Zn3In2S6 composite photocatalysts under mild conditions. International Journal of Hydrogen Energy, 2019, 44, 21803-21820.	3.8	36
45	Remarkable enhancement of photocatalytic performance via constructing a novel Z-scheme KNbO 3 /Bi 2 O 3 hybrid material. Materials Research Bulletin, 2017, 94, 352-360.	2.7	35
46	Revealing the transfer mechanisms of photogenerated charge carriers over g-C3N4/ZnIn2S4 composite: A model study for photocatalytic oxidation of aromatic alcohols with visible light. Journal of Catalysis, 2021, 401, 149-159.	3.1	32
47	The preparation and characterization of composite bismuth tungsten oxide with enhanced visible light photocatalytic activity. CrystEngComm, 2013, 15, 7943.	1.3	31
48	One-pot synthesis of Schiff base compounds <i>via</i> photocatalytic reaction in the coupled system of aromatic alcohols and nitrobenzene using CdIn ₂ S ₄ photocatalyst. Dalton Transactions, 2018, 47, 10915-10924.	1.6	30
49	Visible-light photocatalytic activity and mechanism of novel AgBr/BiOBr prepared by deposition-precipitation. Science Bulletin, 2012, 57, 2901-2907.	1.7	28
50	Tunable photocatalytic and photoelectric properties of I ^{â^'} -doped BiOBr photocatalyst: dramatic pH effect. RSC Advances, 2016, 6, 15525-15534.	1.7	28
51	Synergistic Effect of Photocatalyst CdS and Thermalcatalyst Cr ₂ O ₃ -Al ₂ O ₃ for Selective Oxidation of Aromatic Alcohols into Corresponding Aldehydes. ACS Applied Materials & Interfaces, 2020, 12, 2531-2538.	4.0	26
52	Synthesis of BiPO4 by crystallization and hydroxylation with boosted photocatalytic removal of organic pollutants in air and water. Journal of Hazardous Materials, 2020, 399, 122999.	6.5	26
53	A Novel <scp>CdS</scp> /gâ€ <scp>C₃N₄</scp> Composite Photocatalyst: Preparation, Characterization and Photocatalytic Performance with Different Reaction Solvents under Visible Light Irradiation. Chinese Journal of Chemistry, 2017, 35, 217-225.	2.6	25
54	Ethylene glycol-assisted synthesis, photoelectrochemical and photocatalytic properties of BiOI microflowers. Science Bulletin, 2014, 59, 3420-3426.	1.7	24

#	Article	IF	CITATIONS
55	Amino acid-assisted synthesis of In ₂ S ₃ hierarchical architectures for selective oxidation of aromatic alcohols to aromatic aldehydes. RSC Advances, 2017, 7, 6457-6466.	1.7	22
56	Efficient H ₂ evolution on Co ₃ S ₄ /Zn _{0.5} Cd _{0.5} S nanocomposites by photocatalytic synergistic reaction. Inorganic Chemistry Frontiers, 2022, 9, 1943-1955.	3.0	22
57	Sulfur Vacancy-Mediated Electron–Hole Separation at MoS ₂ /CdS Heterojunctions for Boosting Photocatalytic N ₂ Reduction. ACS Applied Energy Materials, 2022, 5, 4475-4485.	2.5	22
58	THE GREEN PHOSPHOR SrAl ₂ O ₄ : Eu ²⁺ , R ³⁺ (R = Y , Dy) AND ITS APPLICATION IN ALTERNATING CURRENT LIGHT-EMITTING DIODES. Functional Materials Letters, 2013, 06, 1350047.	0.7	21
59	Novel I-BiOBr/BiPO ₄ heterostructure: synergetic effects of I ^{â^²} ion doping and the electron trapping role of wide-band-gap BiPO ₄ nanorods. RSC Advances, 2016, 6, 55755-55763.	1.7	20
60	Novel NiO/RP composite with remarkably enhanced photocatalytic activity for H2 evolution from water. International Journal of Hydrogen Energy, 2021, 46, 19363-19372.	3.8	19
61	Coordinating ultra-low content Au modified CdS with coupling selective oxidation and reduction system for improved photoexcited charge utilization. Journal of Catalysis, 2021, 402, 72-82.	3.1	19
62	Efficient photocatalytic H2 production coupling with selective oxidation of aromatic alcohol under carbon neutrality. Applied Catalysis B: Environmental, 2021, 298, 120619.	10.8	18
63	Construction of NiP _x /MoS ₂ /NiS/CdS composite to promote photocatalytic H ₂ production from glucose solution. Journal of the American Ceramic Society, 2021, 104, 5307-5316.	1.9	17
64	Fe Doped Ni ₃ S ₂ Nanosheet Arrays for Efficient and Stable Electrocatalytic Overall Urea Splitting. ACS Applied Energy Materials, 2022, 5, 1183-1192.	2.5	17
65	Photocatalytic Reduction of Nitro Compounds Using TiO ₂ Photocatalyst by UV and Vis Dyeâ€sensitized Systems. Chinese Journal of Chemistry, 2011, 29, 399-404.	2.6	16
66	The temperatureâ€sensitive luminescence of (Y,Gd)VO ₄ :Bi ³⁺ ,Eu ³⁺ and its application for stealth antiâ€counterfeiting. Physica Status Solidi - Rapid Research Letters, 2012, 6, 321-323.	1.2	16
67	The red luminescence of Sr4 Al14 O25 :Mn4+ enhanced by coupling with the SrAl2 O4 phase in the 3SrO · 5Al2 O3 system. Physica Status Solidi (A) Applications and Materials Science, 2013, 210, 1791	-1798.	16
68	An elemental S/P photocatalyst for hydrogen evolution from water under visible to near-infrared light irradiation. Chemical Communications, 2019, 55, 13160-13163.	2.2	16
69	Fabrication of Z-Scheme WO3/KNbO3 Photocatalyst with Enhanced Separation of Charge Carriers. Chemical Research in Chinese Universities, 2020, 36, 901-907.	1.3	14
70	Preparation, characterisation and activity evaluation of CaCO ₃ /ZnO photocatalyst. Journal of Experimental Nanoscience, 2011, 6, 324-336.	1.3	9
71	Unexpected formation of scheelite-structured Ca1â^'xCdxWO4 (0 ≤ ≤) continuous solid solutions with tunable photoluminescent and electronic properties. Physical Chemistry Chemical Physics, 2017, 19, 23204-23212.	1.3	9
72	Sodium titanate nanowires as a stable and easily handled precursor for the shape controlled synthesis of TiO2and their photocatalytic performance. CrystEngComm, 2014, 16, 616-626.	1.3	8

#	Article	IF	CITATIONS
73	Hydrogenation of Cinnamaldehyde to Hydrocinnamyl Alcohol on Pt/Graphite Catalyst. ChemistrySelect, 2019, 4, 2018-2023.	0.7	8
74	Novel noble-metal free S/Ni12P5/Cd0.5Zn0.5S composite with enhanced H2 evolution activity under visible light. International Journal of Hydrogen Energy, 2020, 45, 33623-33633.	3.8	7
75	Fabrication of Ag/RP composite with excellent photocatalytic activity for degrading high concentration of methyl orange solution. Materials Letters, 2020, 268, 127612.	1.3	7
76	Photothermal synergy of 1D Cd0.9Zn0.1S and 3D Mn3O4 for achieving forcefully active and highly selective aromatic alcohol oxidation. Applied Surface Science, 2022, 579, 151978.	3.1	6
77	Preparation and characterisation of AgIn(WO ₄) ₂ photocatalyst with high photoreduction activity. Journal of Experimental Nanoscience, 2012, 7, 98-108.	1.3	4
78	Wide spectral photocatalytic hydrogen evolution of elemental red phosphorus supported with Au nanoparticles. Catalysis Communications, 2021, 149, 106197.	1.6	4
79	Interaction between CO–Ar–Molten Steel Flow and Decarburization Reaction in Rheinstahl–Heraeus. Steel Research International, 2021, 92, 2100032.	1.0	4
80	Deep Insight into the Pinch Effect in a Tundish with Channelâ€Type Induction Heater. Steel Research International, 2022, 93, .	1.0	4
81	Recent advances in special morphologic photocatalysts for NOx removal. Frontiers of Environmental Science and Engineering, 2022, 16, 1.	3.3	4
82	Synthesis of novel morphology-controlled Bi(OH)CrO4 with high visible light photocatalytic activity. Materials Research Bulletin, 2013, 48, 3292-3297.	2.7	3
83	Inclusion Behavior in a Curved Bloom Continuous Caster with Mold Electromagnetic Stirring. Metals, 2020, 10, 1580.	1.0	3
84	Effect of Nonequilibrium Decarburization on Inclusion Transfer During Single Snorkel RH Vacuum Refining. Jom, 2022, 74, 1578-1587.	0.9	2
85	A NEW RED PHOSPHOR OF THE Mn ACTIVATED NON-STOICHIOMETRIC STRONTIUM ALUMINATE 3SrO•5Al2O3 FOR HIGH COLOR RENDERING WHITE LEDS. Functional Materials Letters, 2013, 06, 1350028.	⁸ 0.7	1